Uncoupling Protein 1 Is Necessary for Norepinephrine-Induced Glucose Utilization in Brown Adipose Tissue

Ken-ichi Inokuma,[1] Yuko Ogura-Okamatsu,[1] Chitoku Toda,[1] Kazuhiro Kimura,[1] Hitoshi Yamashita,[2] and Masayuki Saito[1]

Sympathetic stimulation activates glucose utilization in parallel with fatty acid oxidation and thermogenesis in brown adipose tissue (BAT) through the β-adrenergic receptors. To clarify the roles of the principal thermogenic molecule mitochondrial uncoupling protein 1 (UCP1) in the sympathetically stimulated glucose utilization, we investigated the uptake of 2-deoxyglucose (2-DG) into BAT and some other tissues of UCP1-knockout (KO) mice in vivo. In wild-type (WT) mice, administration of norepinephrine (NE) accelerated the disappearance of plasma 2-DG and increased 2-DG uptake into BAT and heart without any rise of plasma insulin level. In UCP1-KO mice, the stimulatory effect of NE on 2-DG uptake into BAT, but not into heart, disappeared completely. Insulin administration increased 2-DG uptake into BAT and also heart similarly in WT and UCP1-KO mice. NE also increased the activity of AMP-activated protein kinase (AMP kinase) in BAT of WT but not UCP1-KO mice. Our results, together with reports that the activation of AMP kinase increases glucose transport in myocytes, suggest that the sympathetically stimulated glucose utilization in BAT is due to the serial activation of UCP1 and AMP kinase. *Diabetes* 54:1385–1391, 2005

Brown adipose tissue (BAT) is a tissue specified for metabolic heat production, at least in small rodents, during cold acclimation, spontaneous hyperphagia, arousal from hibernation, and recovery from anesthetic hypothermia (1). BAT thermogenesis is principally dependent on the activation of uncoupling protein 1 (UCP1), which uncouples oxidative phosphorylation in mitochondria to dissipate the electrochemical gradient as heat. BAT thermogenesis is directly regulated by sympathetic nerves distributed abundantly to this tissue. The cellular events associated with sympathetic activation of BAT thermogenesis are the binding of norepinephrine (NE) released from sympathetic nerve terminal to β-adrenergic receptor, the activation of adenylate cyclase, and increased hydrolysis of triglyceride. The released fatty acids activate UCP1 and are oxidized in mitochondria to serve as an energy source of thermogenesis. Thus, the principal substrate for BAT thermogenesis is considered to be fatty acids derived from triglycerides in this tissue and also from blood lipoproteins. Together with fatty acids, glucose may be important fuel in BAT, probably not as a direct substrate of thermogenesis but as a carbon source for fatty acid synthesis and rapid oxidation of fatty acids (2,3). Indeed, it has been reported that glucose utilization in BAT is markedly enhanced in parallel with heat production after cold exposure, sympathetic nerve stimulation, and β-adrenergic agonist administration in vivo (4–10). A parallel increase of glucose utilization with thermogenesis was also confirmed in brown adipocytes in vitro (11–13).

In BAT, as in white adipose tissue (WAT) and other insulin-sensitive tissues, glucose utilization is activated by insulin. However, there has been evidence suggesting that the β–adrenergically activated glucose utilization is independent of the action of insulin. For example, exposure of rats to a cold environment for several hours promptly increases 2-deoxyglucose (2-DG) uptake into BAT but not into WAT and skeletal muscle, while it decreases plasma insulin levels (8). In agreement with this in vivo observation, Marette and Bukowiecki (11,12) demonstrated in isolated brown adipocytes that NE could enhance glucose transport predominantly via a β-adrenergic pathway even in the absence of insulin. Moreover, the NE-induced 2-DG uptake into rat brown adipocyte primary culture is not suppressed by wortmannin, an inhibitor of phosphatidylinositol 3-kinase, which is indispensably involved in the signaling pathway for insulin-stimulated glucose transport (14). Very recently, however, Chernogubova et al. (13) reported that NE-induced glucose transport in mouse brown adipocytes was suppressed by a phosphatidyinositol 3-kinase inhibitor (LY294002), suggesting significant involvement of a same downstream signal transduction pathway stimulated by insulin. Shimizu et al. (15) reported that the NE-induced increase in glucose transport in brown adipocytes is attributable to the enhancement of the functional activity of GLUT1 but not to the translocation of GLUT4 to the plasma membrane. In contrast,

From the [1]Department of Biomedical Sciences, Graduate School of Veterinary Medicine, Hokkaido University, Sapporo, Japan; and the [2]Department of Molecular Genetics, National Institute for Longevity Sciences, Obu, Japan.

Address correspondence and reprint requests to Masayuki Saito, PhD, Department of Biomedical Sciences, Graduate School of Veterinary Medicine, Hokkaido University, Sapporo 060-0818, Japan. E-mail: saito@vetmed.hokudai.ac.jp.

Received for publication 24 November 2004 and accepted in revised form 17 February 2005.

2-DG, 2-deoxyglucose; AMP kinase, AMP-activated protein kinase; BAT, brown adipose tissue; FFA, free fatty acid; NE, norepinephrine; UCP, uncoupling protein; WAT, white adipose tissue.

Omatsu-Kanbe and Kitasato (16) reported that NE and insulin independently induced both an increase in transport activity of plasma membrane fraction and a decrease in that of microsomal fraction, suggesting NE-induced translocation of GLUTs into the plasma membrane. An increased recruitment of GLUTs into the plasma membrane was also shown in BAT of cold-adapted rats (9).

There have thus been conflicting reports about the mechanism of β–adrenergically activated glucose utilization. Moreover, an important question remains to be answered about the causal relation between the glucose utilization and thermogenesis in BAT. That is, is glucose utilization increased as a consequence of activated thermogenesis or in parallel with thermogenesis independently? To address this, in the present study, we estimated in vivo glucose utilization in BAT and some other insulin-sensitive tissues of UCP1-knockout (KO) mice, measured 2-DG uptake into individual tissues, and compared the effects of NE and insulin. Our results suggest the β–adrenergically stimulated glucose utilization is primarily dependent on the activation of UCP1 and AMP-activated protein kinase (AMP kinase).

RESEARCH DESIGN AND METHODS

UCP1-KO (*ucp1-/-*) mice on a congenic background of C57BL/6J were generated by backcross matings of heterozygous (+/-) mice on a mixed 129/SvPas and C57BL/6J background with C57BL/6J mice 15 times (17,18), which were kindly given by Dr. L. Kozak (Pennington Biomedical Research Center, Baton Rouge, LA). All wild-type (WT; *ucp1*+/+) mice were C57BL/6J. They were housed in plastic cages at 26°C with a 12-h light-dark cycle (lights on at 0700–1900) and given free access to laboratory diet and water. Male mice weighing 23–33 g were used for experiments at the age of 12–42 weeks. The experimental procedures and care of animals were approved by the animal care and use committee of Hokkaido University.

Thermogenic responses. BAT thermogenic activity was assessed by measuring the temperature changes in BAT and the rectum, as described previously (19). Briefly, overnight-fasted mice were anesthetized with urethan (1.3 g/kg, i.p.), and a small incision was made above the scapula, and the interscapular brown fat pads were partially separated from the muscle below, with the vasculature and nerve supplies to the pads being left intact. Then, mice were placed on a heat plate, and a plastic-coated thermistor of a diameter of 1 mm was placed under the fat pads. Another thermistor was also inserted into the rectum, and the plate was heated gently. After the rectal temperature reached a steady level at ~37°C, NE (0.2 mg/kg) or insulin (1.0 unit/kg) was injected intraperitoneally, and the temperature changes were monitored for 20 min.

2-DG uptake. Tissue glucose utilization was assessed in vivo by measuring tissue uptake of 2-DG according to the procedure described by Hom et al., (20) with slight modifications (4,21). Briefly, overnight-fasted mice were anesthetized with pentobarbital (50 mg/kg, i.p.) and implanted with a polyethylene catheter in the right jugular vein. They were placed on a plate heated gently so that their rectal temperature was kept at ~37°C, and blood samples were taken from the tail vein. Then, 10 ml/kg saline, 0.2 mg/kg NE (Sigma-Aldrich, St. Louis, MO), or 1.0 unit/kg insulin (Novo Nordisk, Bagsvaerd, Denmark) was injected intraperitoneally, and 2-[^{3}H]DG (100 μCi/kg; American Radiolabeled Chemicals, St. Louis, MO) and [^{14}C]sucrose (10 μCi/kg; American Radiolabeled Chemicals) were injected into the jugular vein. Blood samples were taken at 3, 5, 7, 9, and 11 min from the tail vein and diluted with the appropriate volume of heparinized saline to prepare plasma samples. The animals were decapitated at 11 min, and the brain, heart, liver, skeletal muscle (gastrocnemius), epididymal WAT, interscapular BAT, and blood were quickly taken, and 50–300 mg of each tissue specimen was solubilized in 1 ml of 1 N NaOH at 100°C for 15 min. After adding 0.5 ml of 2.2 N perchloric acid, the solution was centrifuged, and the radioactivities of ^{3}H and ^{14}C of the resulting supernatant were measured in a liquid scintillation fluid. The radioactivity in plasma samples was also measured. The plasma concentrations of 2-[^{3}H]DG were plotted on a semilogarithmic scale, and the disappearance rate constant (K_p) was calculated from the slope obtained by a linear regression analysis of the data. The extracellular volume of each tissue was estimated using [^{14}C]sucrose as an extracellular marker and served for calculating the intracellular 2-[^{3}H]DG concentration (4). Briefly, the extracellular volume (μl/mg) was calculated by dividing ^{14}C (dpm/mg tissue) by ^{14}C (dpm/μl plasma) at the time of death (11 min). The concentration of extracellular 2-[^{3}H]DG (dpm/mg tissue) could then be obtained by multiplying the extracellular volume by the concentration of 2-[^{3}H]DG (dpm/μl plasma) at 11 min. Finally, this extracellular concentration of 2-[^{3}H]DG was subtracted from the total tissue concentration to give the intracellular concentration of 2-[^{3}H]DG (dpm/mg tissue). The rate constant of net tissue uptake of 2-[^{3}H]DG was determined using the following equation: $K_i = (Ci_t \times K_p)/(Cp_0 \times ([1 - e^{-Kp \cdot t}])$, where Ci_t is the intracellular 2-[^{3}H]DG concentration at 11 min, K_p is the rate constant of plasma 2-[^{3}H]DG disappearance described above, Cp_0 is the extrapolated plasma 2-[^{3}H]DG concentration at time 0, and t is the duration (11 min). Although the rate constant K_i itself is not a function of blood glucose concentration, it is not a strictly quantitative index of tissue glucose utilization, unless some correction factors for the analogue effect of 2-DG compared with glucose in the transport and phosphorylation steps are determined. Despite these limitations, we assessed tissue glucose utilization from K_i because results of K_i have been confirmed to correspond qualitatively to the known physiological characteristics of the tissues studied. The plasma concentrations of glucose (Glucose B-test Wako; Wako Pure Chemical, Osaka, Japan), free fatty acids (FFA) (nonesterified fatty acid C-test WAKO; Wako Pure Chemical), and insulin (Insulin ELISA kit; Morinaga, Yokohama, Japan) before and 11 min after the hormone injection were also measured.

AMP kinase assay. Overnight-fasted mice were anesthetized and injected with NE (0.2 mg/kg, i.p.) or saline as described above, and 11 min later they were killed by cervical dislocation and quickly frozen in liquid nitrogen. Tissue specimen (20–50 mg) of interscapular BAT was homogenized in a buffer containg 50 mmol/l Tris-HCl (pH 7.5), 0.25 mol/l mannitol, 1 mmol/l EGTA, 1 mmol/l EDTA, 1 mmol/l dithiothreitol, 50 mmol/l sodium fluoride, 5 mmol/l sodium pyrophosphate, 1 mmol/l phenylmethylsulfonyl fluoride, 1 mmol/l benzamidine, and 4 μg/ml soybean trypsin inhibitor and centrifuged at 14,000*g* for 20 min at 4°C. The resultant supernatant was treated with polyethylene glycol 8,000 (Wako Pure Chemical) as described (22), and the pellet fraction obtained after 6% polyethylene glycol 8,000 treatment was used for AMP kinase assay. AMP kinase activity was assessed by measuring the incorporation of ^{32}P from [γ-^{32}P]ATP into a synthetic SAMS peptide (Upstate, Charlottesville, VA) for 5 min in the presence and absence of 0.2 mmol/l AMP (22).

The contents of α-catalytic subunit and the phosphorylated form of AMP kinase in BAT were determined by Western blotting, using antibodies against α-subunit of AMP kinase (Cell Signaling Technology, Beverly, MA) and its phosphorylated form at Thr-172 (Cell Signaling Technology). Two micrograms of the pellet fraction obtained after 6% polyethylene glycol 8,000 treatment mentioned above were separated by SDS-PAGE and transferred onto polyvinylidine fluoride membranes (Immobilon; Millipore, Bedford, MA). The membranes were incubated overnight in a blocking buffer (20 mmol/l Tris-HCl [pH 7.5], 150 mmol/l NaCl) containing 0.1% Tween 20 and 5% skimmed milk and then in the buffer containing each antibody overnight. The bound antibody was made visible using horseradish peroxidase–linked goat anti-rabbit immunoglobulin (Zymed Laboratories, San Francisco, CA) and an enhanced chemiluminescence system (Amersham, Little Chalfont, Bucks, U.K.). The intensity of chemiluminescence for the corresponding bands was analyzed by the National Institutes of Health Image Public Domain Image Processing and Analysis program (National Institutes of Health; available at http://rsb.info.nih.gov/nih-image/).

mRNA expression. Total RNA was prepared from adipose tissues with the use of TRIZOL (Invitrogen, Carlsbad, CA) according to manufacture's protocol, and mRNA levels of UCP1, -2, and -3; GLUT1 and -4; and glyceraldehyde 3-phosphate dehydrogenase were quantified by real-time RT-PCR. Briefly, 2 μg of total RNA was reverse transcripted with an oligo (dT) 15-adaptor primer and Maloney murine leukemia virus reverse transcriptase (Invitrogen). Real-time PCR was performed on a fluorescence thermal cycler (Light Cycler System; Roche Diagnostics, Mannheim, Germany), using Sybr Green I as a double-strand DNA–specific dye according to manufacture's protocol. Primers used were 5′-GTG AAG GTC AGA ATG CAA GC-3′ and 5′-AGG GCC CCC TTC ATG AGG TC-3′ for mouse UCP1, 5′-GGC TGG TGG TGG TCG GAG AT-3′ and 5′-CCG AAG GCA GAA GTG AAG TG-3′ for mouse UCP2, 5′-GAG CGG ACC ACT CCA GCG TC-3′ and 5′-TGA GAC TCC AGC AAC TTC TC-3′ for mouse UCP3, 5′-GCT TCC TGC TCA TCA ATC GTA AC-3′ and 5′-CTC GAA GAT GCT CGT TGA GTA GT-3′ for mouse GLUT1, 5′-CAC AGA AGG TGA TTG AAC AGA GC-3′ and 5′-AAG ACA TTG TTG GCC AGC ATAG C-3′ for mouse GLUT4, and 5′-GAA GGT CGG TGT GAA CGG ATT-3′ and 5′-GAA GAC ACC AGT AGA CTC CAC GAC ATA-3′ for mouse glyceraldehyde 3-phosphate dehydrogenase.

Data analysis. All values are expressed as means ± SE. Statistical analysis was performed using one-way ANOVA. Significant differences were determined using the Dunnett's test for comparison with control and the Tukey-Kramer HSD test for multiple comparisons.

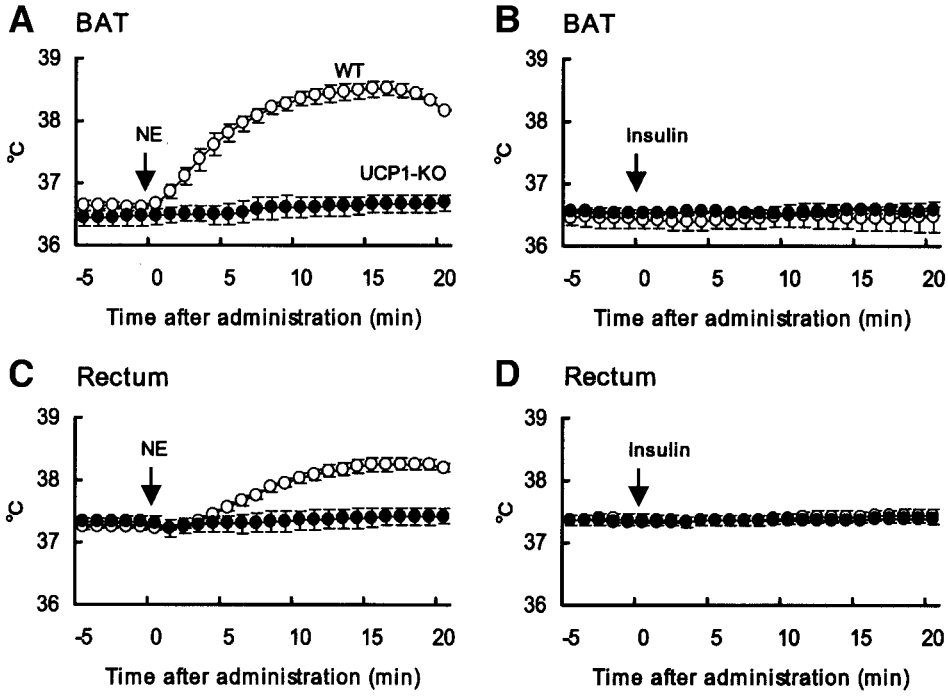

FIG. 1. Thermogenic activity of WT and UCP1-KO mice. WT (○) and UCP1-KO (●) mice were anesthetized (urethane, 1.3 g/kg), and temperature changes of interscapular BAT (*A* and *B*) and rectum (*C* and *D*) were monitored after intraperitoneal injection of NE (0.2 mg/kg; *A* and *C*) and insulin (1.0 unit/kg, *B* and *D*). Values are means ± SE for three mice.

RESULTS

Thermogenic acitivity of BAT. The interscapular BAT of UCP1-KO mice weighed more, looked paler, and had enlarged intracellular lipid droplets compared with that of WT mice, as reported previously (17). To confirm the impaired thermogenic activity of BAT of UCP1-KO mice, first we monitored temperature changes in the interscapular BAT and the rectum after intraperitoneal injection of NE and insulin (Fig. 1). Although the basal temperature of the BAT and rectum did not differ between UCP1-KO and WT mice, BAT temperature was slightly lower than rectal temperature in all mice. In WT mice, NE injection elicited a rapid rise in BAT temperature followed by a gradual rise in rectal temperature. In contrast, in UCP1-KO mice, the temperature responses were much less. Insulin injection did not produce any consistent temperature changes in the BAT and also in the rectum for at least 20 min. These results clearly indicate that the sympathetically activated thermogenesis by BAT is markedly impaired in UCP1-KO mice.

2-DG disappearance from blood and 2-DG uptake in BAT and other tissues. Tissue glucose utilization was assessed from the rate constant of tissue 2-DG uptake calculated from the intracellular concentrations of 2-[^{3}H]DG and the disappearance rate of 2-[^{3}H]DG from blood. Plasma 2-DG disappeared exponentially at the rate constant of 0.037–0.039 min^{-1} (Fig. 2). NE or insulin injection tended to increase the disappearance rate of plasma 2-DG in both WT and UCP1-KO mice.

In BAT of WT mice, the rate constant of 2-DG uptake was 0.0058 ± 0.0006 min^{-1} in saline controls and increased more than twofold after NE and insulin injections, 0.0131 ± 0.0019 and 0.0124 ± 0.0022 min^{-1}, respectively (Fig. 3). In BAT of UCP1-KO mice, the rate constant with saline injection (0.0093 ± 0.0011 min^{-1}) was higher than those in BAT of WT mice and increased about twofold after insulin injection, while it did not change at all after NE injection.

The rate constant of 2-DG uptake was also calculated for the brain, heart, liver, epididymal WAT, and skeletal muscle (gastrocnemius). As shown in Fig. 4, in WT mice, NE increased the rate constant in the heart but not in the other tissues examined, while insulin increased those in

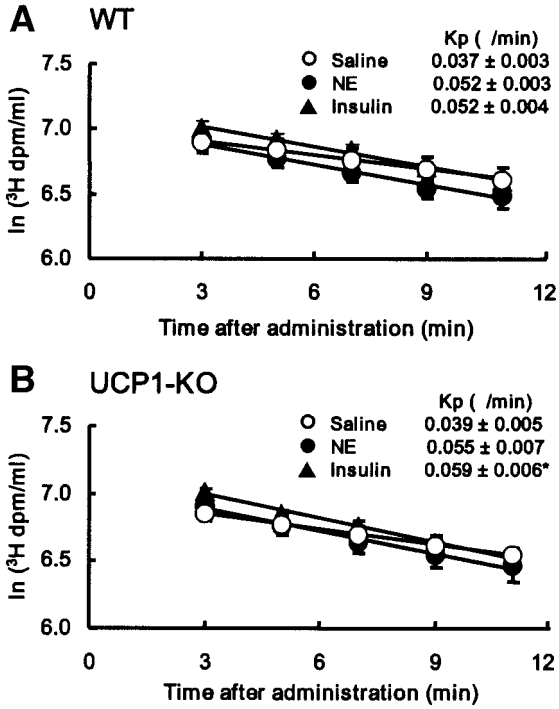

FIG. 2. Disappearance of 2-[^{3}H]DG from plasma. WT (*A*) and UCP1-KO (*B*) mice were fasted overnight, anesthetized, injected with NE (0.2 mg/kg, ●), insulin (1.0 unit/kg, ▲), or saline (○) intraperitoneally, and 2-[^{3}H]DG was injected into the jugular vein at time 0. Blood samples were taken from the tail vein at 2-min intervals, and the 2-[^{3}H]DG radioactivity in plasma was measured. The disappearance rate constant (K_p) of 2-[^{3}H]DG was calculated from a linear regression line for ln[2-[^{3}H]DG] vs. time. Values are means ± SE for 4–7 mice. *$P < 0.05$ vs. saline controls.

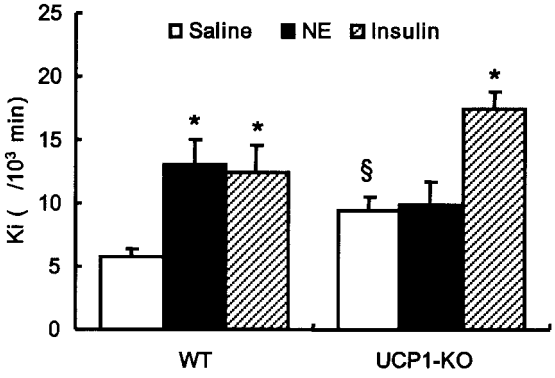

FIG. 3. 2-DG uptake into interscapular BAT. WT and UCP1-KO mice were treated as in Fig. 2 and decapitated at 11 min, and radioactivities of 2-[^{3}H]DG and [^{14}C]sucrose in interscapular BAT were measured. The rate constant of the net 2-[^{3}H]DG uptake (K_i) was calculated from the intracellular concentration and plasma disappearance rate constant of 2-[^{3}H]DG. Values are means ± SE for 4–7 mice. *P < 0.05 vs. saline controls; §P < 0.05 vs. WT mice.

the heart and WAT. Neither NE nor insulin affected the rate constant in the brain and liver. The 2-DG uptake into the skeletal muscle was too low to calculate the rate constant accurately. The rate constant of 2-DG uptake into the individual tissues of UCP1-KO mice, together with the effects of NE and insulin, was almost similar to those in WT mice. Thus, the stimulatory effect of NE on 2-DG uptake into BAT, but not into heart, disappeared in UCP1-KO mice, while the effect of insulin was not influenced in BAT and also in some insulin-sensitive tissues.

Plasma glucose, FFA, and insulin. The changes of plasma glucose, FFA, and insulin concentrations, together with 2-[^{3}H]DG in plasma, were examined after the injection of either NE or insulin. As shown in Table 1, when vehicle was injected, neither glucose, FFA, nor insulin concentration changed in 11 min. NE injection significantly increased plasma glucose and FFA concentrations but did not change plasma insulin concentrations. Insulin injection decreased plasma glucose and FFA concentrations. There was no significant difference in the effects of NE and insulin between UCP1-KO and WT mice.

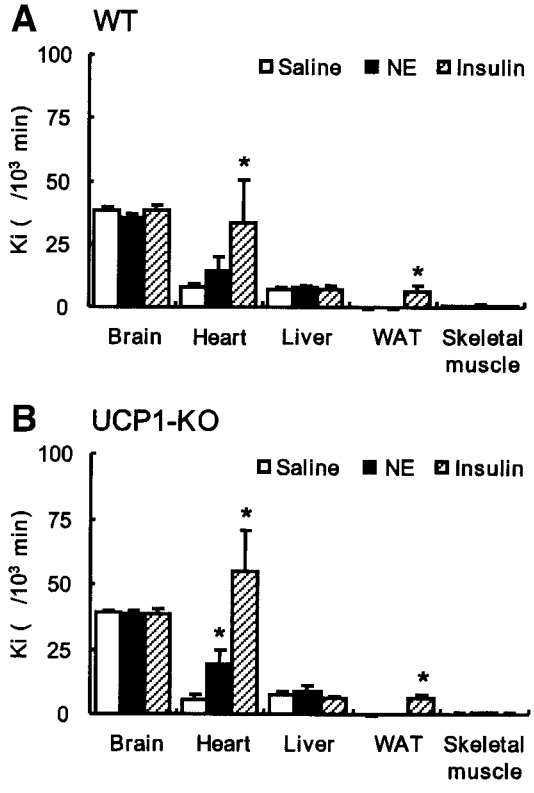

FIG. 4. 2-DG uptake into brain, heart, liver, epididymal WAT, and skeletal muscle (gastrocnemius). WT (*A*) and UCP1-KO (*B*) mice were treated as in Fig. 2, and the K_i value of each tissue was calculated as in Fig. 3. Values are means ± SE for 4–7 mice. *P < 0.05 vs. saline controls.

AMP kinase activity. There has been growing evidence for the role of AMP kinase in insulin-independent glucose utilization seen during anoxia and exercise (24–26). We also examined the effect of NE on AMP kinase activity in BAT of WT and UCP1-KO mice. As shown in Fig. 5, NE injection into WT mice produced about a twofold increase in the AMP kinase activity in BAT regardless of the presence and absence of AMP. In contrast, NE showed no significant effect on the AMP kinase activity in BAT of UCP1-KO mice. Quite similar effects of NE were also observed for the content of the phosphorylated form, an active form of this enzyme, of AMP kinase. That is, NE doubled phosphorylation of AMP kinase in WT mice without any changes in total content of AMP kinase protein, whereas it had no significant effect in UCP1-KO mice.

mRNA expression of UCP and GLUT. The mRNA expression levels of individual isoforms of UCP and GLUT in the interscapular BAT were measured by the quantitative real-time RT-PCR method and normalized by those of glyceraldehyde 3-phosphate dehydrogenase. UCP1 mRNA was detected in WT BAT but not in UCP1-KO BAT, as expected. In contrast, UCP2 mRNA levels were 2.3 times higher in UCP1-KO mice. There was no difference in UCP3 mRNA levels between the two types of mouse. These results on UCP mRNA expression in UCP1-KO mice were well consistent with those reported previously (17). GLUT1 mRNA levels were 1.4 times higher in UCP1-KO mice. However, there was no significant difference in GLUT4 mRNA levels between UCP1-KO and WT mice.

DISCUSSION

To clarify the causal relationship between the adrenergic activation of glucose utilization and thermogenesis in BAT, we used UCP1-KO mice, which have been proven to lack β–adrenergically activated thermogenesis and to be cold intolerant (17,18). In fact, we confirmed that the BAT and rectal temperature increased in minutes after NE administration in WT but not UCP1-KO mice. The mRNA levels of UCP2 and UCP3 in BAT were increased and unchanged, respectively, in UCP1-KO mice compared with WT mice. Thus, it seems unlikely that these two UCP isoforms play significant roles in NE-activated thermogenesis in BAT. The principal findings of the present study were *1*) intraperitoneal administration of NE, as well as insulin, increased 2-DG uptake into BAT and heart of WT mice, *2*) the NE-stimulated 2-DG uptake in BAT disappeared in UCP1-KO mice, *3*) insulin increased 2-DG uptake in BAT similarly in the WT and UCP1-KO mice, *4*) the stimulatory effects of NE and insulin in the heart were similar in both types of mouse, and *5*) NE increased the

TABLE 1
Changes in plasma concentrations of glucose, FFA, and insulin after NE or insulin injection

	WT		KO	
	0 min	11 min	0 min	11 min
Plasma glucose (mg/dl)				
Vehicle	127 ± 12	122 ± 9	113 ± 7	113 ± 7
NE	121 ± 16	155 ± 10*	119 ± 12	171 ± 24*
Insulin	118 ± 6	89 ± 4*	115 ± 8	89 ± 10*
Plasma FFA (μEq/l)				
Vehicle	885 ± 100	734 ± 23	924 ± 153	804 ± 87
NE	1,076 ± 13	1,231 ± 37*	955 ± 150	1,211 ± 67
Insulin	1,107 ± 82	645 ± 29*	951 ± 69	618 ± 59*
Plasma insulin (ng/ml)				
Vehicle	0.33 ± 0.04	0.27 ± 0.08	0.26 ± 0.06	0.21 ± 0.04
NE	0.32 ± 0.02	0.25 ± 0.05	0.23 ± 0.02	0.22 ± 0.10
Insulin	0.22 ± 0.06	3.27 ± 0.65*	0.22 ± 0.10	3.62 ± 0.54*

Data are means ± SE for 3 mice. WT and UCP1-KO mice were fasted overnight, anesthetized, and injected with 0.2 mg/kg NE, 1.0 unit/kg insulin, or saline intraperitoneally as vehicle as in Fig. 2. The concentration of plasma glucose, FFA, and insulin were measured before and 11 min after the injection. *$P < 0.05$ vs. 0 min.

activity of AMP kinase in BAT of WT but not UCP1-KO mice.

In most previous studies about in vivo glucose utilization in BAT, the rat was used as a model animal, probably because of appropriate body size. One exception was, as far as we know, that of Cooney et al. (10,23), who used mice and demonstrated marked increases in 2-DG uptake in BAT and heart by intravenous administration of insulin or NE. Our present results also confirmed the stimulatory effects of NE and insulin in 2-DG uptake into BAT and heart of overnight WT mice. It is to be noted, however, that our results were different in some aspects from those of Cooney et al. (10,23); for example, the rate constant of tissue 2-DG uptake was much lower, and the stimulatory effects of insulin and NE were weaker. These would be due to the differences in the feeding condition and the route of hormone administration. That is, we injected NE or insulin intraperitoneally to overnight-fasted mice, while they injected intravenously to fed or 3- to 4-h–fasted mice. Moreover, in the present study, 2-DG uptake into the skeletal muscle and WAT were very low, and stimulatory effects of insulin were undetectable in skeletal muscle. Although the precise reasons are not known at present, this may be attributable, at least in part, to the relatively weak dose response of 2-DG uptake to insulin in skeletal muscle compared with heart and BAT (23). That is, the plasma insulin concentrations after intraperitoneal injection (Table 1) might be too low to substantially stimulate 2-DG uptake into skeletal muscle. More important findings were that the stimulatory effect of NE was almost abolished in UCP1-KO mice. This may not be due to some defect of the glucose transport/metabolism pathway itself, because 2-DG uptake at the basal condition without stimulation was higher in UCP1-KO mice than WT mice. Indeed, the mRNA expression levels of GLUT1 and -4 were rather higher and similar, respectively, in UCP1-KO mice. Moreover, in contrast with NE, insulin increased 2-DG uptake into BAT about twofold in both UCP1-KO and WT mice. All these results collectively indicate that the NE-stimulated 2-DG uptake into BAT is mostly dependent on the activation of UCP1 but independent of the insulin-stimulated mechanism.

How does UCP1 activation increase glucose utilization in BAT? Although we cannot answer this question in detail, is seems intriguing to compare with glucose utilization induced by exercise and anoxia in muscle, which is also independent of insulin action (24,25). There are now various lines of evidence for a critical role of AMP kinase, which is activated synergistically by AMP and phosphorylation, in the insulin-independent glucose transport (24). For example, glucose transport into muscle is increased when treated with either an AMP analogue, 5-aminoimidazole-4-carboxamide 1-β-D-ribonucleoside, which activates AMP kinase, or a constitutively active (dominant-positive) AMP kinase but decreased with a dominant-negative AMP kinase (26,27). Moreover, AMP kinase activation induces the recruitment of GLUT4 to the plasma membrane (27). All these facts support a view that muscle contraction and/or anoxia produce a decreased cellular energy status with increased AMP-to-ATP ratio, which leads to AMP kinase activation and finally increased glucose transport via GLUT4. Phosphatidyinositol 3-kinase–independent glucose transport and GLUTs translocation were also reported in myotubes treated with dinitrophenol, a chemical uncoupler of mitochondrial oxidative phosphorylation (28). Accordingly, a similar scenario may be applicable to BAT. In fact, we found in the present study that NE increased the activity and the phosphorylated form of AMP kinase in BAT of WT but not of UCP1-KO mice. Moreover, NE stimulation produces a drop of cellular ATP levels and a rise of AMP levels in brown adipocytes in vitro (29) and also in BAT in vivo (M.S., K.I., Y.O-O., C.T., K.K., H.Y., unpublished observations), probably because of uncoupling of mitochondrial oxidative phosphorylation by UCP1. The stimulatory effects of UCP1 on AMP kinase and glucose utilization were also demonstrated in skeletal muscle ectopically expressing UCP1 (30,31). Thus, it is most likely that stimulation of BAT with NE results in UCP1 activation, which leads to AMP kinase activation and finally increased glucose uptake.

What is the physiological relevance of the UCP1-dependent glucose utilization in BAT? In connection with the putative mechanism noted above, it seems most rational to consider it as a compensatory phenomenon for rapid recovery of cellular energy charge (ATP levels) by activating anaerobic glycolysis. Increased glycolysis may also be

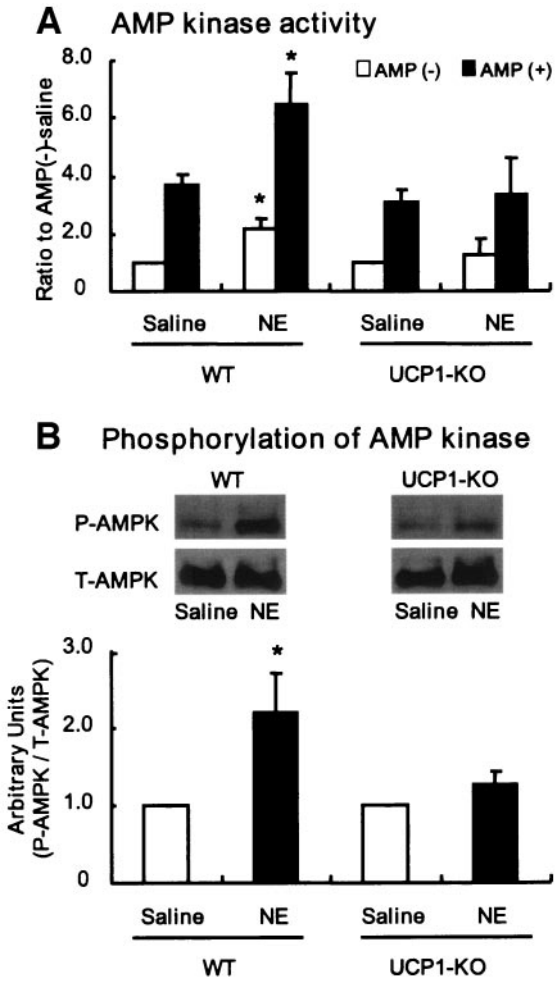

FIG. 5. AMP kinase activity of interscapular BAT. WT and UCP1-KO mice were anesthetized as in Fig. 2, injected with NE (0.2 mg/kg) or saline intraperitoneally, and decapitated 11 min later. *A*: AMP kinase activity in an extract of interscapular BAT was measured in the presence (■) and absence (□) of 0.2 mmol/l AMP and expressed as relative to the basal activity of saline control in the absence of AMP (0.06 ± 0.02 and 0.12 ± 0.04 nmole · min^{-1} · mg^{-1} protein for WT and UCP1-KO mice, respectively). *B*: The same tissue extract was analyzed by Western blotting to detect phosphorylated and total AMP kinase using specific antibodies. The amount of phosphorylated form (P-AMPK) was normalized by those of total AMP kinase (T-AMPK) and expressed as relative to those of saline controls of respective mice. Values are means ± SE for 3–5 mice. *$P < 0.05$ vs. saline controls.

favorable for sufficient supply of oxaloacetate to enable rapid oxidation of fatty acids and acetyl CoA by the citric acid cycle. Regardless of these possibilities, it is to be noted that respiratory uncoupling by UCP1 is indeed one of the mechanisms responsible for an insulin-independent increase in tissue glucose utilization. This suggests that activation and/or increased expression of UCP1 may ameliorate impaired glucose metabolism caused by insulin resistance. In the present study, no notable difference was found in the disappearance rate of 2-DG from blood between WT and UCP1-KO mice. This may imply minor contribution of the UCP1-dependent glucose uptake to the whole-body glucose utilization in mice expressing medial amounts of UCP1. However, there have been reports demonstrating improved glucose tolerance in mice expressing increased amounts of UCP1 not only in adipose tissues (32,33) but also in skeletal muscle (30,31). Moreover, Bukowiecki and colleagues (4,34) have shown that insulin sensitivity is increased in rats acclimated to cold environments and chronically treated with NE, both of which induce UCP1 in BAT and WAT. Thus, UCP1 activation may improve glucose utilization not only by its unique insulin-independent mechanism discussed above but also synergistically with the insulin-dependent mechanisms.

ACKNOWLEDGMENTS

This study was supported by a grant-in-aid for scientific research from the Ministry of Education, Culture, Sports, Science and Technology of Japan.

We thank Dr. L. Kozak (Pennington Biomedical Research Center, Baton Rouge, LA) for providing us with UCP1-KO mice.

REFERENCES

1. Cannon B, Nedergaard J: Brown adipose tissue: function and physiological significance. *Physiol Rev* 84:277–359, 2004
2. Isler D, Hill HP, Meier MK: Glucose metabolism in isolated brown adipocytes under beta-adrenergic stimulation: quantitative contribution of glucose to total thermogenesis. *Biochem J* 245:789–793, 1987
3. McCormack JG: The regulation of fatty acid synthesis in brown adipose tissue by insulin. *Prog Lipid Res* 21:195–223, 1982
4. Vallerand AL, Perusse F, Bukowiecki LJ: Cold exposure potentiates the effect of insulin on in vivo glucose uptake. *Am J Physiol* 253:E179–E186, 1987
5. Shibata H, Perusse F, Vallerand A, Bukowiecki LJ: Cold exposure reverses inhibitory effects of fasting on peripheral glucose uptake in rats. *Am J Physiol* 257:R96–R101, 1989
6. Vallerand AL, Perusse F, Bukowiecki LJ: Stimulatory effects of cold exposure and cold acclimation on glucose uptake in rat peripheral tissues. *Am J Physiol* 259:R1043–R1049, 1990
7. Shimizu Y, Nikami H, Saito M: Sympathetic activation of glucose utilization in brown adipose tissue in rats. *J Biochem* 110:688–692, 1991
8. Shimizu Y, Saito M: Activation of brown adipose tissue thermogenesis in recovery from anesthetic hypothermia in rats. *Am J Physiol* 261:R301–R304, 1991
9. Greco-Perotto R, Zaninetti D, Assimacopoulos-Jeannet F, Bobbioni E, Jeanrenaud B: Stimulatory effect of cold adaptation on glucose utilization by brown adipose tissue: relationship with changes in the glucose transporter system. *J Biol Chem* 262:7732–7736, 1987
10. Cooney GJ, Caterson ID, Newsholme EA: The effect of insulin and noradrenaline on the uptake of 2-[1-^{14}C]deoxyglucose in vivo by brown adipose tissue and other glucose-utilising tissues of the mouse. *FEBS Lett* 188:257–261, 1985
11. Marette A, Bukowiecki LJ: Noradrenaline stimulates glucose transport in rat brown adipocytes by activating thermogenesis: evidence that fatty acid activation of mitochondrial respiration enhances glucose transport. *Biochem J* 277:119–124, 1991
12. Marette A, Bukowiecki LJ: Stimulation of glucose transport by insulin and norepinephrine in isolated rat brown adipocytes. *Am J Physiol* 257:C714–C721, 1989
13. Chernogubova E, Cannon B, Bengtsson T: Norepinephrine increases glucose transport in brown adipocytes via beta3-adrenoceptors through a cAMP, PKA, and PI3-kinase-dependent pathway stimulating conventional and novel PKCs. *Endocrinology* 145:269–280, 2004
14. Shimizu Y, Shimazu T: Effects of wortmannin on increased glucose transport by insulin and norepinephrine in primary culture of brown adipocytes. *Biochem Biophys Res Commun* 202:660–665, 1994
15. Shimizu Y, Satoh S, Yano H, Minokoshi Y, Cushman SW, Shimazu T: Effects of noradrenaline on the cell-surface glucose transporters in cultured brown adipocytes: novel mechanism for selective activation of GLUT1 glucose transporters. *Biochem J* 330:397–403, 1998
16. Omatsu-Kanbe M, Kitasato H: Insulin and noradrenaline independently stimulate the translocation of glucose transporters from intracellular stores to the plasma membrane in mouse brown adipocytes. *FEBS Lett* 314:246–250, 1992
17. Enerback S, Jacobsson A, Simpson EM, Guerra C, Yamashita H, Harper ME, Kozak LP: Mice lacking mitochondrial uncoupling protein are cold-sensitive but not obese. *Nature* 387:90–94, 1997
18. Hofmann WE, Liu X, Bearden CM, Harper ME, Kozak LP: Effects of genetic

background on thermoregulation and fatty acid-induced uncoupling of mitochondria in UCP1-deficient mice. *J Biol Chem* 276:12460–12465, 2001
19. Saito M, Minokoshi Y, Shimazu T: Brown adipose tissue after ventromedial hypothalamic lesions in rats. *Am J Physiol* 248:E20–E25, 1985
20. Hom FG, Goodner CJ, Berrie MA: A [^{3}H]2-deoxyglucose method for comparing rates of glucose metabolism and insulin responses among rat tissues in vivo: validation of the model and the absence of an insulin effect on brain. *Diabetes* 33:141–152, 1984
21. Kraegen EW, James DE, Jenkins AB, Chisholm DJ: Dose-response curves for in vivo insulin sensitivity in individual tissues in rats. *Am J Physiol* 248:E353–E362, 1985
22. Kudo N, Barr AJ, Barr RL, Desai S, Lopaschuk GD: High rates of fatty acid oxidation during reperfusion of ischemic hearts are associated with a decrease in malonyl-CoA levels due to an increase in 5′-AMP-activated protein kinase inhibition of acetyl-CoA carboxylase. *J Biol Chem* 270: 17513–17520, 1995
23. Cooney GJ, Astbury LD, Williams PF, Caterson ID: Inuslin response in individual tissues of control and gold thioglucose-obese mice in vivo with [1-^{14}C]2-deoxyglucose. *Diabetes* 36:152–158, 1987
24. Goodyear LJ, Kahn BB: Exercise, glucose transport, and insulin sensitivity. *Annu Rev Med* 49:235–261, 1998
25. Hardie DG: The AMP-activated protein kinase cascade: the key sensor of cellular energy status. *Endocrinology* 144:5179–5183, 2003
26. Mu J, Brozinick JT Jr, Valladares O, Bucan M, Birnbaum MJ: A role for AMP-activated protein kinase in contraction- and hypoxia-regulated glucose transport in skeletal muscle. *Mol Cell* 7:1085–1094, 2001
27. Russell RR 3rd, Bergeron R, Shulman GI, Young LH: Translocation of myocardial GLUT-4 and increased glucose uptake through activation of AMPK by AICAR. *Am J Physiol* 277:H643–H649, 1999
28. Tsakiridis T, Vranic M, Klip A: Phosphatidylinositol 3-kinase and the actin network are not required for the stimulation of glucose transport caused by mitochondrial uncoupling: comparison with insulin action. *Biochem J* 309:1–5, 1995
29. Pettersson B, Vallin I: Norepinephrine-induced shift in levels of adenosine 3′:5′-monophosphate and ATP parallel to increased respiratory rate and lipolysis in isolated hamster brown-fat cells. *Eur J Biochem* 62:383–390, 1976
30. Li B, Nolte LA, Ju JS, Han DH, Coleman T, Holloszy JO, Semenkovich CF: Skeletal muscle respiratory uncoupling prevents diet-induced obesity and insulin resistance in mice. *Nat Med* 6:1115–1120, 2000
31. Han DH, Nolte LA, Ju JS, Coleman T, Holloszy JO, Semenkovich CF: UCP-mediated energy depletion in skeletal muscle increases glucose transport despite lipid accumulation and mitochondrial dysfunction. *Am J Physiol* 286:E347–E353, 2004
32. Tsukiyama-Kohara K, Poulin F, Kohara M, DeMaria CT, Cheng A, Wu Z, Gingras AC, Katsume A, Elchebly M, Spiegelman BM, Harper ME, Tremblay ML, Sonenberg N: Adipose tissue reduction in mice lacking the translational inhibitor 4E-BP1. *Nat Med* 7:1128–1132, 2001
33. Kopecky J, Hodny Z, Rossmeisl M, Syrovy I, Kozak LP: Reduction of dietary obesity in aP2-Ucp transgenic mice: physiology and adipose tissue distribution. *Am J Physiol* 270:E768–E775, 1996
34. Liu X, Perusse F, Bukowiecki LJ: Chronic norepinephrine infusion stimulates glucose uptake in white and brown adipose tissues. *Am J Physiol* 266:R914–R920, 1994